Bulletin of the Seismological Society of America, Vol. 89, No. 1, pp. 156–164, February 1999

Nature of Narrow-Band Signals at 2.083 Hz

by Götz H. R. Bokelmann* and Stefan Baisch

Abstract We study the nature of extremely narrow-band signals that appear in typical long-time spectra of seismic recordings. At the German Experimental Seismic System (GERESS) array, we observe several of these time-continuous spectral lines. The most prominent one has a frequency near 2.083 Hz. The close agreement of this frequency with one of the feasible rotation frequencies of synchronous machines (50 Hz /24) suggests an industrial origin of the signal. An observed signal gap of 11 h duration is thus interpreted as a temporary machine shutdown. Interestingly, the signal vanishes (or is at least strongly reduced in amplitude) in the whole eastern part of the German Regional Seismic Network (GRSN) suggesting (1) that a single source dominates the signal in that region and (2) that the narrow-band signal propagates to distances of more than 300 km. On the other hand, we study the character of the wave by performing a suitably adapted array analysis. Estimates of the propagation direction suggest a source location near the German–Czech border. We obtain an estimate of the apparent velocity near 4 km/sec. Comparison with transient arrivals from regional earthquakes suggests that the narrow-band energy propagates as regional phases of *Lg* and *Sg* type.

Introduction

The character of seismic noise has been studied well before the advent of digital seismology. For example, Frantti (1963) analyzed spectra of seismic noise at various places on the Earth. Besides the general microseismic noise maximum at periods between 3 and 12 sec, there were indications of persistent narrow peaks, particularly in the vicinity of 2 Hz. The frequency range up to a few Hertz was studied using specially designed analog spectral analyzers (Walker *et al.*, 1964). They found sets of extremely narrow-band signals, which persisted up to days. An industrial origin was supposed, because spectral lines started and stopped abruptly.

Douze (1967) analyzed data gathered within boreholes. He found in several cases that, unlike the general noise amplitudes, the narrow-band signals did not decay with depth and were thus easily detected at greater depth, down to the maximum survey depth of 2900 m. Nevertheless, it was impossible to explain the character of the wave.

The behavior of the signal at 25 stations distributed over Germany was studied by Steinwachs (1974). Based on the apparent global occurrence of the signal, he discussed a possible extraterrestric origin through gravitational waves generated by a pulsar. For the short time windows of 20 sec he used, no frequency variations could be resolved. Such variations were, however, found by Hjortenberg and Risbo (1975), thus excluding a pulsar as the source. Instead, they found a hydroelectric power plant, which caused a signal at 2.78 Hz. The frequency varied slightly, in close association with the frequency of the power network. However, the frequency variation of the equally prominent signal at 2.083 Hz showed no relation with the power network frequency. Hjortenberg and Risbo (1975) and Bungum *et al.* (1977) suggested that the source of the latter signal is located at some greater distance.

Plesinger and Wielandt (1972, 1974) found a strong peak near 2.1 Hz. They were able to separate the peak into two subpeaks, one at a stable frequency and the other at a frequency that varies with time. The same patterns were found in the network frequencies of the western and the eastern European power network, respectively. In addition, they identified a large piston compressor as a possible source for elastic waves for the western European network component. Their observations suggest that the wave could propagate to distances of at least several hundred kilometers, the distance of the Czech border to the station BUH in the Black Forest in southwestern Germany. The Czech Republic is the closest country that was connected to the eastern European network.

This article addresses the nature of the narrow-band signal at 2.083 Hz through the use of an extended seismic network, the German Regional Seismic Network (GRSN), which consists of 15 broadband stations distributed over Germany. We study the amplitude behavior within and outside a signal gap, in which the machine giving rise to the

*Present address: Department of Geophysics, Stanford, California 94305-2215.

signal is apparently switched off. The extent of the spatial area, in which the signal amplitude drops significantly, gives us clues about the propagation distance of the wave. The second line of argument comes from array analysis of the signal at the short-period regional GERESS array and a temporary short-period array operated at the site of the Kontinentale Tiefbohrung (KTB). Estimates of propagation direction suggest an approximate location of the source while estimates of propagation velocity can be used to determine the dominant wave propagation mode.

Observations

The GERESS array is a short-period regional array located in southeastern Bavaria near the Czech border. Technical details are given in Harjes (1990). Figure 1 shows the power density spectrum of a long time series of one of the GERESS stations (not corrected for system response). Such spectra typically show the strong maximum near 0.2 Hz (microseismicity), the instrumentally caused sharp decay at lower frequency and the smoother decay to higher frequency, corresponding to a frequency dependence of noise ground displacement as f^{-4}. A typical feature of long-time spectra at most sites, not only at the GERESS array, is the occurrence of additional narrow peaks, which we call *spectral lines.* In the figure, these lines are compared with possible rotation frequencies (network frequency divided by the number of pole pairs) of machines running synchronously with the German power network (Rentzsch, 1968) that operates at a frequency of 50 Hz (or 16⅔ Hz for the German railway system). Several of these rotation frequencies, shown by broken lines and a circle at the top, are observed in the seismic data. The frequency of the strongest spectral line in the data closely matches the rotation frequency at 50 Hz /24 [or (16⅔) Hz /8] suggesting that one or more of such machines give rise to this spectral line. However, synchronous machines apparently do not cause all of these spectral lines, because many other lines are not associated with any of the rotation frequency.

In principle, spectral peaks can arise from processing artifacts, such as insufficient smoothing or improper windowing of the data. In this case, however, the peak at 50/24 Hz is in fact highly significant. More important, perhaps, is the evolution of the spectral lines with time. Figure 2 shows a sonogram for a longer time window of 6 days. The spectral lines show up as horizontal lines in the figure. Most notably, the strongest spectral line has a remarkable continuity with time, beside a gap on the fourth day, where the signal appears to vanish for about 11 h. There are indications of temporal persistence also for several other spectral lines. However, this type of display does not allow inferences about weaker spectral lines. Vertical lines result from regional and teleseismic events, with the former showing up at higher frequency than the latter. Also apparent is the night and day difference in background noise. Because this difference does not show on the second day, a Sunday, the day and night

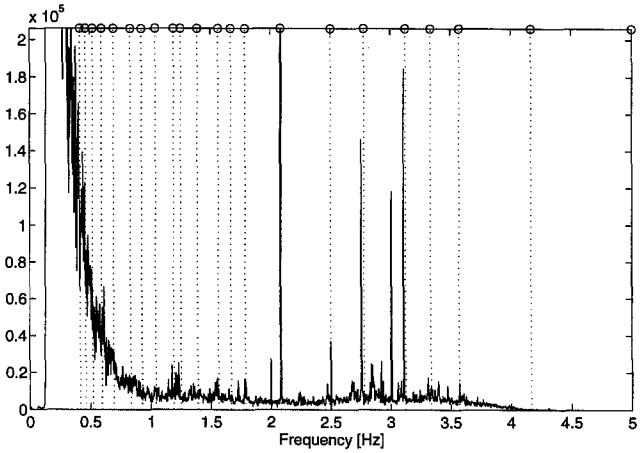

Figure 1. Noise power density spectrum of raw short-period data recorded by GERESS station D3. Note the extremely narrow-band spectral lines. Data length is 1 h starting at midnight on 19 April 1997. Subwindow length is 512 data points resampled at Δt = 0.1 sec; Hanning window is used with 50% overlap. The y axis gives counts^2 * sec. Further descriptions are given in the text.

difference in background noise level is clearly due to man-made influences.

In the following, we will focus on the spectral line at 50/24 Hz, in particular, the signal gap on the fourth day. We use stations of the GRSN, all of which consist of Streckeisen STS-2 instruments and Quanterra data loggers (Hanka, 1990). Figure 3 gives the location of the 16 GRSN stations together with the GERESS array. The spectral line at 50/24 Hz is observed at most stations with low background noise amplitude. Signal amplitudes vary between 0.2 and 0.6 nm ground displacement. It is quite remarkable that this small sinusoidal ground displacement of only few atomic radii can in fact be measured. The low-amplitude level contrasts somewhat with the observation by Plesinger and Wielandt (1974) more than 20 years ago for station KHC (60 km north of GERESS): They found a (half-)amplitude of 4 nm for the spectral line at that frequency. If we are dealing with the same signal, then the signal amplitude has weakened substantially in the meantime.

Stations with higher background noise level (BRNL, RGN, IBBN, FUR, BUG, STU) do not show a distinct peak in the time windows selected. However, another time window with particularly low background noise level suggested distinct peaks also at stations STU and IBBN.

In comparison, Figure 4 shows the result for a time window within the 11-h signal gap. Signal amplitudes in the eastern part of the network are either dramatically weakened or have vanished entirely (empty circles). Because the gap is during daytime, the background noise level is increased but certainly not enough to mask an outside-the-gap-signal amplitude (beside station GRF). Whatever caused the line spectrum in the eastern part of the network, it affected all of

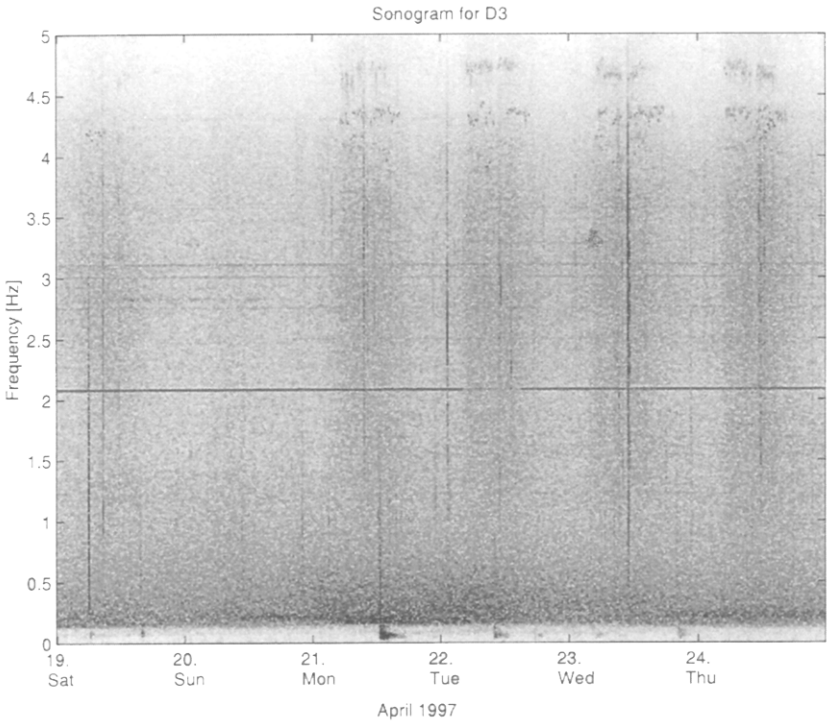

Figure 2. Frequency content of raw data at station D3 as a function of time for 6 days. No normalization is used. The subwindow length is 2 min. Only every 10th time window is displayed. The prominent narrow-band signal (spectral line) near 2.1 Hz is observed continuously except for an 11-h gap on the fourth day. Vertical lines are caused by regional and teleseismic events. Note that this type of display may mask weaker spectral lines.

those stations! This suggests the presence of a single strong source in the eastern part, because different machines are expected to be shut down independently.

In contrast, the amplitudes in the western part of the network do not seem to be affected significantly. The relatively strong signal at TNS has not weakened in fact. It even seems slightly stronger, as do the observations at GSH and BFO. This suggests that at least one other source is located in the western part, perhaps close to station TNS. These sources do not show the signal gap.

Array Analysis

So far, we have used individual stations of the network for the analysis only. However, complementary information about the presence and location of the source(s) can be obtained by adapting array analysis techniques to the case of nearly monochromatic signals. A seismological array such as GERESS (Fig. 5), with its 25 vertical-component instruments, allows the determination of arrival direction and apparent velocity for plane-wave arrivals. In addition, the five three-component instruments can be used to study the polarization behavior of the wave.

The technique we adapted for the narrow-band signals is based on the multiple signal classification analysis technique (MUSIC) (Schmidt, 1981; Goldstein and Archuleta, 1987). Details are given in the Appendix. For a 1-h time window, the MUSIC objective function reaches a maximum at an apparent velocity of 4 ± 0.7 km/sec and a backazimuth of $348° \pm 12°$. As a formal error is difficult to specify for MUSIC, we take the half-width as a conservative estimate of uncertainty.

Figure 3 also displays backazimuths resulting from array analysis of the two short-period arrays: (1) GERESS array and (2) a temporary array at the site of the Kontinentale Tiefbohrung Oberpfalz. The signal arrival direction at the GERESS array is 348°. Outside of the signal gap, this backazimuth estimate is remarkably stable: Results of the array analysis for a succession of 4-h time windows (Fig. 6) show consistent patterns outside the gap and a single dominant signal (eigenvalue), while no coherent arrival can be found within the gap.

Besides the GERESS array, only one other suitable array data set in the area is available to us, namely, the temporary array at the Kontinentale Tiefbohrung Oberpfalz (KTB; Zoback and Harjes, 1997). We applied the same array analysis to five subarrays out of six, which gave consistent results during localization of local seismic events. Figure 3 shows the scatter of backazimuths (one standard deviation) determined by these five subarrays. The scatter is larger than the resulting uncertainty from GERESS, most likely due to the smaller size of the KTB subarrays and the temporary installation compared with the permanent GERESS installation in vaults.

The intersection of arrival directions from GERESS and KTB suggests a source location near the northern border of Czechia with Germany. A source location in that general area appears reasonable also by comparison of Figures 3 and 4. During the machine shutdown (Fig. 4), all stations within 300 km of this location showed a sharply reduced signal amplitude or no signal at all.

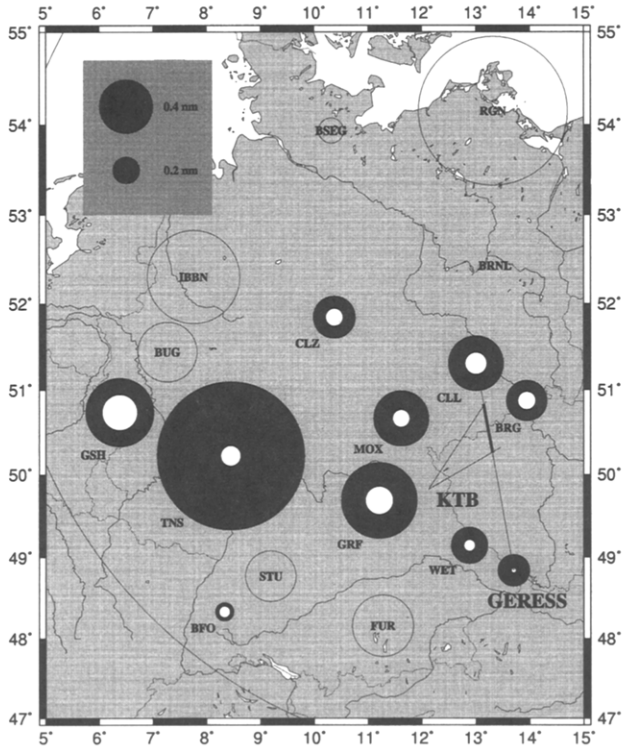

Figure 3. Strength of the 50/24 Hz signal at the GRSN stations and GERESS averaged over three 15-min time windows outside the signal gap (in nm). Black circles give the average signal amplitude. For comparison with the background noise level, white circles give the corresponding average amplitude in four nearby frequency bands at ± 0.05 and ± 0.1 Hz. Empty circles give the noise amplitude at stations where no narrow peak was observed at 50/24 Hz. Lines at the GERESS and KTB arrays give estimates of arrival directions.

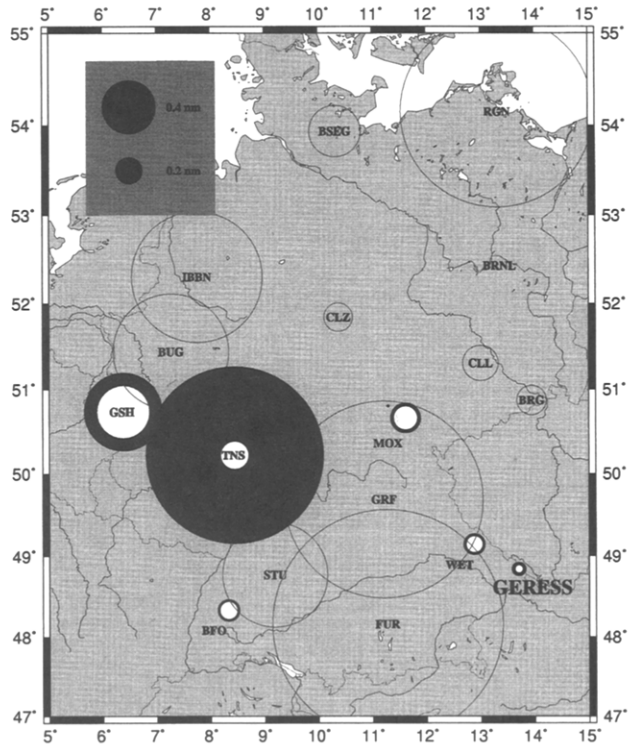

Figure 4. Same as Figure 3, but for a time window within the 11-h signal gap. Note that the signal amplitude is reduced or missing on all of the eastern stations but is still apparent in the western part of the network.

Regional-Wave Propagation

We have obtained an estimate of apparent velocity from the GERESS array of 4 km/sec for the 2.083-Hz signal. Such estimates are crucial to narrow down the wave type and, respectively, the wave path of the dominant energy of the signal (Backus *et al.,* 1964). In principle, the energy propagates as body waves of *P*- and *S*-wave types and as surface waves. But which propagation mode carries most of the energy?

To answer that question, we might resort to modeling the wave propagation through a regional Earth model. However, simple tests showed that amplitudes of regional phases depend strongly on details of the velocity-depth function (e.g., Mendi *et al.,* 1997). Thus, we take the approach of simply comparing with apparent velocities of regional phases observed at GERESS after regional seismic events.

Table 1 gives locations and further specifications of two events used in this study. The distances of the events range from 330 to 590 km. The events have local magnitudes M_L

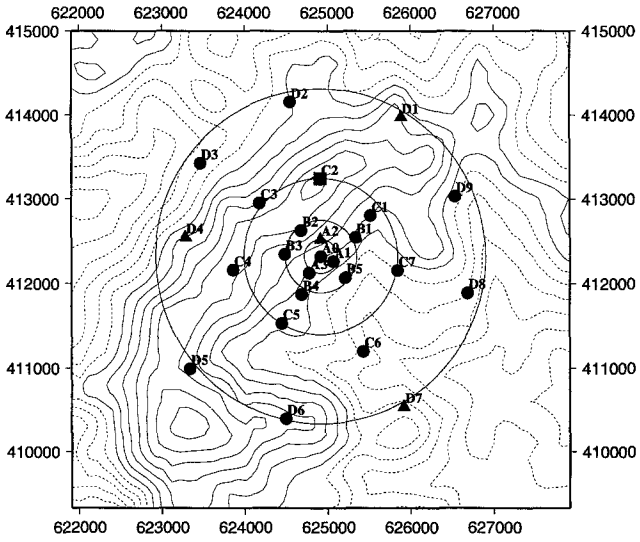

Figure 5. Array configuration of the GERESS array in southeastern Bavaria. The 25 vertical short-period channels are shown by filled circles. Filled triangles show sites of three-component instruments; the square shows a site of an additional broadband instrument. The aperture is about 4 km (units are m, with Gauss–Krüger coordinates). Topographic contours are at 20-m intervals.

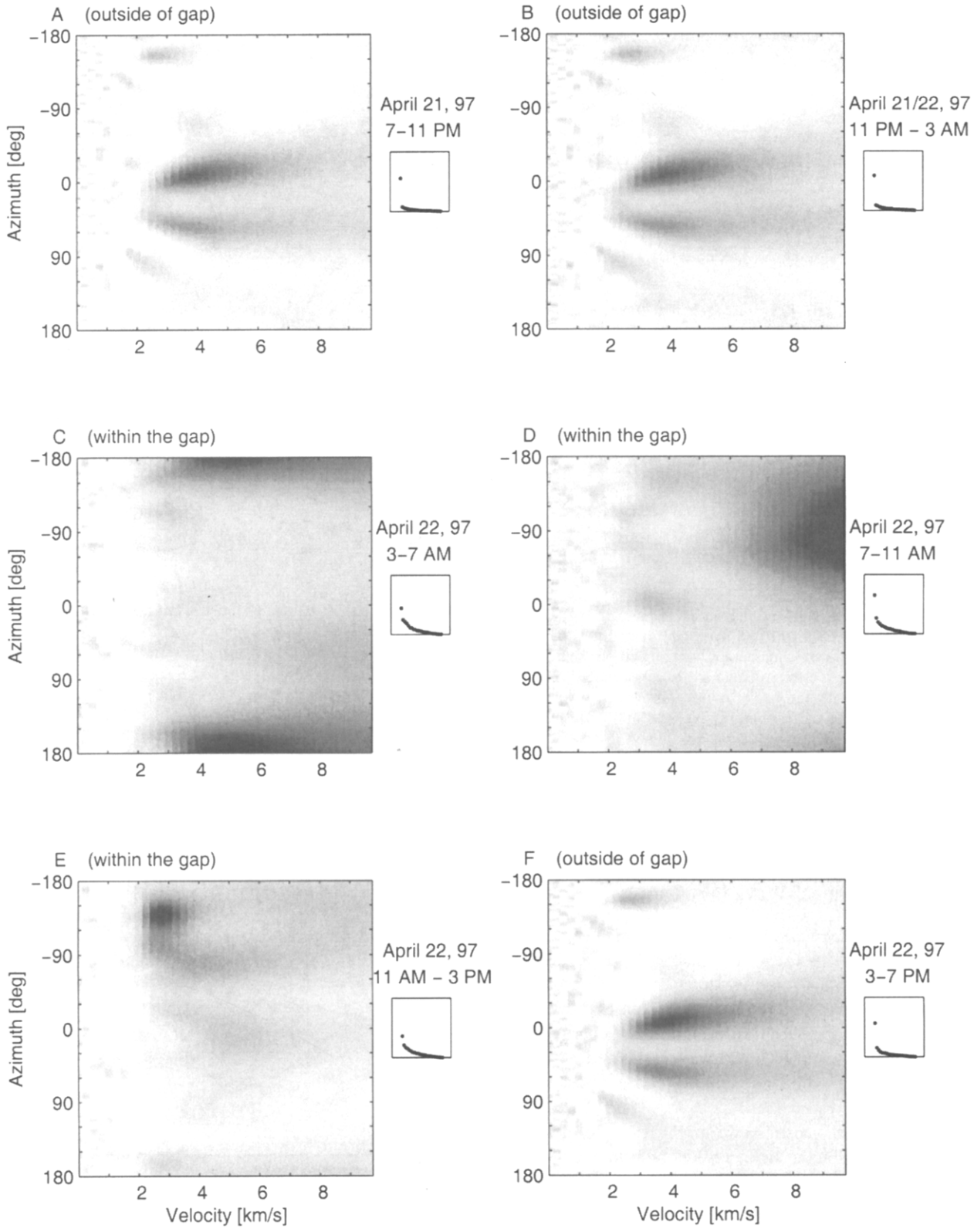

Figure 6. Array analysis results for a number of successive 4-h time windows across the signal gap. Dark shades indicate high values of the MUSIC objective function. Windows A, B, and F are outside the gap, while C, D, and E are within. The small windows give the size of the eigenvalues, suggesting a single dominant signal. Within the gap, the results change substantially from time window to time window, indicating the absence of coherent arrivals.

Table 1
Locations and Specifications of Two Events

Event	Date	Time	Latitude	Longitude	Depth	M_L	Region	Type
1	09.09.91	18:36:57.0	51.414	16.220	1	3.2	Lubin, Poland	mining event
2	29.05.91	20:24:40.4	45.016	8.213	10	3.8	Northern Italy	earthquake

of 3.2 and 3.8 and have thus relative high dominant frequencies of several Hertz. Figure 7 gives the associated seismograms recorded at GERESS.

Figure 7a shows a mining event from Lubin (event 1). The beginning of the seismogram shows apparent velocities above 8 km/sec, which is consistent with *P*-wave propagation through the uppermost mantle. As time progresses, apparent velocities decrease somewhat, consistent with a *P*-wave propagation through the crust (e.g., P_g). At about 30 sec, velocity shows an uprupt decrease to values below 6 km/sec (*Sn*). Eventually, velocity drops further to values that scatter around 4 km/sec. We obtain velocities near 4 km/sec for the arrivals carrying the strongest energy, which appear at times near L_g. This pattern is roughly confirmed by the Northern Italian earthquake (event 2).

The agreement of apparent velocities from the dominant regional arrivals and the 2.083-Hz signal suggests that most of the energy generated by the machines at 2.083 Hz propagates as the same wave type as the dominant regional arrivals. These wave types have been identified as shear waves, most notably L_g, which consists of *SH* and *SV* waves propagating through the crust with overcritical reflections at Moho and surface (Bouchon, 1982). The character of L_g has been found to depend substantially on lateral variations in crustal structure. For example, it has been observed to be blocked from passage through heterogeneous regions as graben regions (Mendi *et al.,* 1997). For the GERESS region, it was found that L_g waves have group velocities depending on the backazimuth. For waves arriving from northwestern directions, velocities are higher than for those arriving from southern direction (Jia, 1996). Interestingly, group velocities are somewhat lower than phase velocities. The difference is perhaps due to dispersion, analogously to surface waves.

The regional-wave character indicates why it may be possible to observe the 2.083-Hz signal over substantial distances of several hundred kilometers. Because the wave is trapped within the crust, the amplitude decay with distance can be expected to be weaker than for body waves. Experience at GERESS shows, however, that substantial variations with direction exist. Paths from northern directions (as the 2.083-Hz signal) are much less attenuative than paths from the south (Jia, 1996; Sereno *et al.,* 1992).

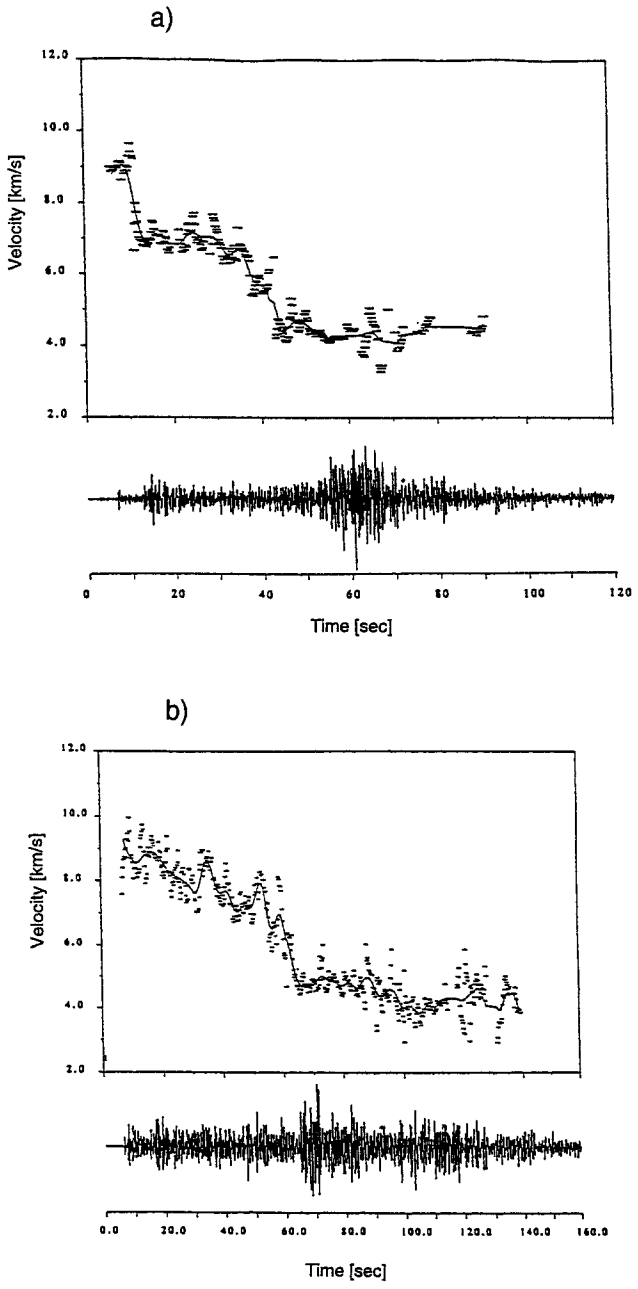

Figure 7. Seismograms of two regional events observed at GERESS and estimates of apparent velocity for a sliding time window of 1.5 sec length and 0.2 sec increment (after Gestermann, 1992). Apparent velocity and seismogram (a) for event 1 (Lubin) and (b) for event 2 (Northern Italy).

Phase and Frequency

Figures 1 and 2 showed the amplitude of the narrow-band signal at GERESS station D3. Now we study the behavior of the associated phase. Figure 8 shows in this respect

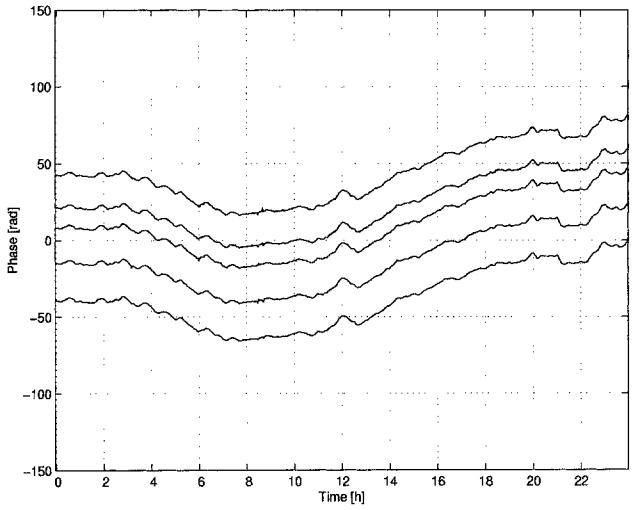

Figure 8. Observations of the phase at the fixed frequency 50/24 Hz at stations D3, D4, D7, D8, and D9 (19 April). The subwindow length is 2 min.

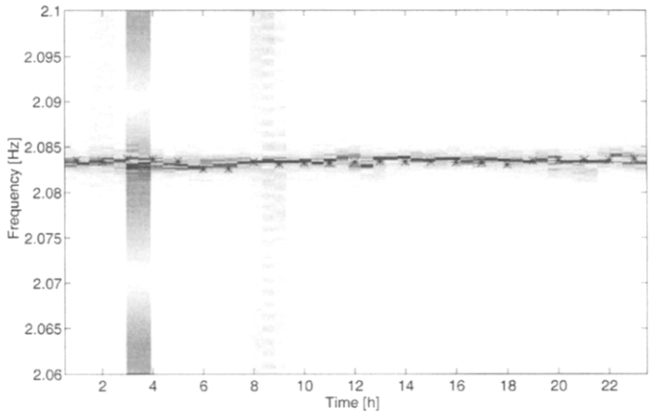

Figure 9. Measurement of center frequency of the spectral peak for the same time window as in Figure 8 using the center of gravity (after Baisch, 1997).

how the phase varies with time, for several of the GERESS D stations. It shows systematic changes, with all stations affected similarly. This can be understood, if the phase changes are primarily due to the source, perhaps by load changes of the source during the day (Rentzsch, 1968). Alternatively, we can interpret these phase changes as temporal changes of frequency. This is illustrated in Figure 9, where the center frequency (center of gravity) is shown as a function of time.

Besides the 25 vertical-component instruments, the GERESS array also had 5 three-component instruments. We found that the polarization differs strongly from station to station, both in direction as well as in degree of ellipticity, although each polarization pattern was quite stable with time. Two colocated instruments gave closely similar results indicating that polarization differences between stations are due to wave propagation characteristics in the subsurface and not to instrument coupling or the instrument itself. A possible cause of the polarization differences is the occurrence of resonances in the subsurface under the stations, which would affect different stations differently. Thus, it seems generally impossible to use polarization to determine the wave type or to determine the backazimuth of the arrival.

Conclusions

We have focused on a narrow-band signal near 50/24 Hz, which is observed in data from many seismological stations in Europe. To infer the wave type and the likely source location, we used data from the GRSN and two small arrays in Bavaria. Within a signal gap, in which the source is apparently switched off, the signal is (at least) greatly reduced in amplitude on all of the eastern stations. Array analysis at GERESS and the temporary KTB array shows that, outside of the signal gap, the wave consists of a single dominant wave front. In the case of GERESS, the wave arrives from 348° with an apparent velocity of 4 km/sec. Together, these pieces of evidence suggest that the observations on the eastern stations are dominated by a single source, which is located near the German–Czech border. At least one more source is located in the western part. Comparison with regional events suggests that the narrow-band energy propagates as a regional shear wave, most likely of L_g type.

The most likely type of source is a machine running synchronously with a power network, either the one at 50 Hz or that of the railway system running at 16 2/3 Hz. Depending on the load, the source phase slows or accelerates with time, which is equivalent to small changes in the radiated frequency.

A signal as the one discussed here may in principle be applied to the monitoring of subtle changes of wave propagation characteristics with time, in particular, wave velocities. Such an analysis would be interesting, because it might give an (indirect) indication of changes in either the stress level within the crust or of changes in the fluid content (see Bokelmann, 1997).

Acknowledgments

We thank H.-P. Harjes, A. Plesinger, E. Wielandt, and W. Zürn for valuable discussions. The suggestion to study the mysterious narrow-band signal at 2.083 Hz came from Rainer Kind. Last but not least, this work would not have been possible without the remarkable effort of the group maintaining the GERESS array, namely, Mike Jost. This study was partly funded by the Deutsche Forschungsgemeinschaft. We gratefully acknowledge comments by Leigh House and an anonymous reviewer.

References

Backus, M., Burg, J., Baldwin, D, Ryan, E., 1964. Wide band extraction of mantle P waves from ambient noise, *Geophys.*, **29,** 672–692.

Baisch, S., 1997. Schmalbandige Signale im GERESS-Rauschspektrum, *Diplomarbeit,* Ruhr-Universität Bochum.

Bokelmann, G. H. R., 1997. Messung zeitlicher Variationen von Wellen-

geschwindigkeiten in der Erdkruste, *Mitt. Deut. Geophys. Ges.*, **3,** 6–12.

Bouchon, M., 1982. The complete synthesis of seismic crustal phases at regional distances, *J. Geophys. Res.*, **87,** B3, 1735–1741.

Bungum, H., Risbo, T., Hjortenberg, E., 1977. Precise continuous monitoring of seismic velocity variations and their possible connection with solid Earth tides, *J. Geophys. Res.*, **82,** 35, 5363–5373.

Douze, E. J., 1967. Short-period seismic noise, *Bull. Seism. Soc. Am.*, **57,** 1, 55–81.

Frantti, G., 1963. The nature of high-frequency earth-noise spectra, *Geophys.*, **28,** 4, 547–562.

Friedlander, B., Weiss., A. J., 1992. Direction finding using spatial smoothing with interpolated arrays, *IEEE Trans. Aerosp. El. Sys.*, **28,** 2, 574–587.

Gestermann, 1992. Characteristics of regional phases recorded at GERESS, in: *Advanced Waveform Research Methods for GERESS Recordings,* DARPA Semiannual Report No. AFOSR 90-0189, April 1992, pp. 60–91.

Goldstein, P., Archuleta, R., 1987. Array analysis of seismic signals, *Geophys. Res. Let.*, **14,** 13–16.

Hanka, W., 1990. The German broadband seismic network (GRN) project. In: *Workshop on Mednet,* Eds: E. Boschi, D. Giardini and A. Morelli, Instituto Nazionale di Geofisica, Roma.

Harjes, H. P., 1990. Design and siting of a new regional array in Central Europe, *Bull. Seism. Soc. Am.*, **80,** 6, 1801–1817.

Hjortenberg, E., Risbo, T., 1975. Monochromatic components of the seismic noise in the Norsar area, *Geophys. J. Roy. Astron. Soc.*, **42,** 547–554.

Jia, Y, 1996. Bestimmung der scheinbaren Dämpfung seismischer Wellen in der europäischen Lithosphäre, *PhD Thesis,* Ber. Inst. Geophys., Ruhr-Universität Bochum, Reihe A, 47.

Mendi, C. D., Ruud, B. O., Husebye, E. S., 1997. The North Sea Lg-blockade puzzle, *Geophys. J. Int.*, **130,** 669–680.

Plesinger, A., Wielandt, E., 1972. Preliminary results of the investigation of the 2 cps ambient earth noise at European sites, Europ. Seism. Soc., Brasov.

Plesinger, A., Wielandt, E., 1974. Seismic noise at 2 Hz in Europe, *J. Geophys.*, **40,** 131–136.

Rentzsch, H., 1968. *Handbuch für Elektromotoren,* Brown Boveri & Cie AG, Mannheim.

Schmidt, R., 1981. A signal subspace approach to multiple emitter location and spectral estimation, *Ph.D. Thesis,* Stanford University, Stanford, California.

Sereno, T. J., Swanger, H. J., Jenkins, R. D., Nagy, W. C., Wahl, D. D., 1992. Attenuation and travel-time characteristics of regional phases recorded at GERESS, *Proceedings of the GERESS Symposium,* June 22–24, 1992, Institute of Geophysics, Ruhr-University Bochum, Germany, 93–102.

Shan, T.-J., Wax, M., Kailath, T., 1985. On spatial smoothing for direction-of-arrival estimation of coherent signals, *IEEE Trans. Acoust. Sp. Sig. Proc.*, **33,** 4, 806–811.

Steinwachs, M., 1974. Systematische Untersuchungen der kurzperiodischen seismischen Bodenunruhe in der Bundesrepublik Deutschland, *Geol. Jb.*, **E3,** Hannover, 59.

Walker, R., Menard, J., Bogert, B., 1964. Real-time high resolution spectroscopy of seismic background noise, *Bull. Seism. Soc. Am.*, **54,** 2, 501–509.

Wax, M., Kailath, T., 1985. Detection of signals by information theoretic criteria, *IEEE Trans. Acoust. Sp. Sig. Proc.*, **33,** 2, 387–392.

Zoback, M., Harjes, H. P., 1997. Injection-induced earthquakes and crustal stress at 9 km depth at the KTB deep drilling site, Germany, *J. Geophys. Res.*, **102,** B8, 18477–18491.

Appendix

Narrow-Band Data Analysis

An approach that is ideally suited to the analysis of narrow-band signals is the multiple signal classification analysis technique (MUSIC). Developed by Schmidt (1981), it was first applied to seismological data by Goldstein and Archuleta (1987). Compared with conventional beamforming techniques, the main advantage of MUSIC is the detectability of monochromatic, stationary signals even at very low signal–noise ratios. That is possible by using long-time averaging to improve the spatial resolution while sacrificing time resolution.

The technique assumes that the observations consist of stationary, monochromatic, complex, plane waves and white noise. Consider q signals observed on an array of N ($N > q$) sensors. Then, the signal vector at station $\mathbf{x}_i$ can be written as

$$\psi(\mathbf{x}_i, t) = \sum_{m=1}^{q} A_m e^{i[\mathbf{k}_m \mathbf{x}_i - \omega t + \phi_m(t)]} + \eta(\mathbf{x}_i, t), \tag{A1}$$

where $\mathbf{k}_m$ and $\phi_m(t)$ are wave vector and phase of the mth signal. $\eta(\mathbf{x}_i,t)$ is a measure of the noise at station $\mathbf{x}_i$.

The cross-spectral matrix (CSM) is defined by

$$R_{ij} = \langle \psi(\mathbf{x}_i, t) \psi^H (\mathbf{x}_j, t) \rangle_t, \tag{A2}$$

where $\langle\ \rangle_t$ denotes time averaging and $(..)^H$ the Hermitian conjugate. If the signals and noise $\eta(\mathbf{x}_i,t)$ are all mutually uncorrelated, the CSM can be written as

$$\mathbf{R} = \mathbf{U}\mathbf{S}\mathbf{U}^H + \sigma^2\mathbf{I}, \tag{A3}$$

where $\mathbf{I}$ is the N-dimensional identity matrix,

$$\mathbf{U} = \begin{bmatrix} e^{i\mathbf{k}_1\mathbf{x}_1} & \cdots & e^{i\mathbf{k}_q\mathbf{x}_1} \\ \vdots & \ddots & \vdots \\ e^{i\mathbf{k}_1\mathbf{x}_N} & \cdots & e^{i\mathbf{k}_q\mathbf{x}_N} \end{bmatrix},$$

and

$$\mathbf{S} = \begin{bmatrix} |A_i|^2 & \cdots & 0 \\ \vdots & \ddots & \vdots \\ 0 & \cdots & |A_q|^2 \end{bmatrix}.$$

The singular value decomposition of $\mathbf{R}$ yields two sets of eigenvectors spanning two orthogonal (signal and noise) subspaces (see Goldstein and Archuleta, 1987):

$$\mathbf{R} = \underbrace{\mathbf{E}_s\mathbf{\Lambda}_s\mathbf{E}_s^H}_{\text{signal}} + \underbrace{\mathbf{E}_n\mathbf{\Lambda}_n\mathbf{E}_s^H}_{\text{noise}}, \tag{A4}$$

$\mathbf{\Lambda}_s$ and $\mathbf{\Lambda}_n$ are diagonal matrices that contain the eigenvalues for the corresponding eigenvectors in $\mathbf{E}_s$ and $\mathbf{E}_n$. The number of present signals q, which specifies the dimension of $\mathbf{E}_s$, can be determined from the cross-spectral matrix using either the AIC or the MDL criterium (Wax and Kailath, 1985).

As a result of the orthogonal structure of $\mathbf{R}$, the mth column of $\mathbf{E}_s$ has the form of the steering vector of the mth signal:

$$\mathbf{a}(\mathbf{k}_m) = [e^{i\mathbf{k}_m\mathbf{x}_1}, \ldots, e^{i\mathbf{k}_m\mathbf{x}_N}]^N. \quad \text{(A5)}$$

Therefore, the q signals can be determined by searching for wave parameters (e.g., apparent velocity and backazimuth) giving rise to optimum fit to the signal covariance $\mathbf{E}_s$. Here, MUSIC involves the search for peaks in

$$D(\mathbf{k}) = \frac{1}{|\mathbf{a}(\mathbf{k}) \cdot \mathbf{E}_n|^2}. \quad \text{(A6)}$$

Exploiting the fact that the signal and noise subspaces are orthogonal, we look for the minimum projection of the steering vector $\mathbf{a}(\mathbf{k})$ onto the noise subspace.

However, the assumptions involved are usually not satisfied by seismic data. We can generate complex signals from real seismograms by constructing the analytic signal. But the assumption of random and uncorrelated phase functions $\phi(t)$ are usually poor approximations to our signals. In that case, the CSM is

$$R_{ij} = \underbrace{\left\langle \sum_{m=1}^{q} A_m^2 e^{i[\mathbf{k}_m(\mathbf{x}_i - \mathbf{x}_j)]} \right\rangle_t}_{\text{signal-covariance}} + \underbrace{\left\langle \sum_{\underbrace{m=1}_{m \neq n}}^{q} \sum_{n=1}^{q} A_m A_n e^{i[\mathbf{k}_m\mathbf{x}_i - \mathbf{k}_n\mathbf{x}_j + \phi_m(t) - \phi_n(t)]} \right\rangle_t}_{\text{signal-correlation}} + \underbrace{\langle \eta(\mathbf{x}_i, t)\eta^H(\mathbf{x}_j, t) \rangle_t}_{\text{noise-covariance}} + \underbrace{\langle \mathrm{CORR}\{\eta(\mathbf{x}_i, t), S_l\} + \mathrm{CORR}\{\eta^H(\mathbf{x}_j, t), S_l\} \rangle_t}_{\text{signal-noise-correlation}}$$

$$l = 1, \ldots, q,$$

where

$$\mathrm{CORR}\{\eta(\mathbf{x}_i, t), S_l\} \equiv \eta(\mathbf{x}_i, t) \sum_{m=1}^{q} A_m e^{i[\omega t - \mathbf{k}_m\mathbf{x}_j - \phi_m(t)]}$$

Deviations from (A3) result if the noise is not necessarily uncorrelated. For large time windows, however, this problem is expected to vanish. Also, the signal–noise correlation terms asymptotically vanish, but not the contributions from correlations between individual signals. For example, two different but perfectly correlated signals give rise to signal correlation terms that are independent of time and are therefore not affected by time averaging. This problem requires preprocessing, namely, array averaging.

For stationary signals in synthetic data, Goldstein and Archuleta (1987) used a spatial averaging technique developed by Shan *et al.* (1985). Unfortunately, this technique is restricted to linear and equidistant arrays, and therefore, it is not easily applicable to seismic arrays of arbitrary geometry. Friedlander and Weiss (1992) combined spatial averaging techniques with array interpolation and made MUSIC applicable for correlated signals with no restrictions on the array geometry. The proposed algorithm includes a linear transformation of the CSM and then applies MUSIC to the transformed CSM. The algorithm requires high numerical accuracy in matrix operations, which is not easily achieved. We obtained much better results using an averaging technique that operates directly on the elements of the CSM.

Here we suggest an approximative spatial averaging technique that simply averages over elements of the CSM (stations pairs), where

$$\Delta\mathbf{x}^{(ij)} = \mathbf{x}_i - \mathbf{x}_j = \text{const} \quad \text{(A7)}$$

approximately holds. It is easy to prove that this averaging affects only the signal correlation term but not the signal covariance. For seismological array geometries like that of GERESS, equation (A7) can only be fulfilled within certain error bounds, which leads to a trade-off between the number of station pairs and the spatial resolution due to the signal covariance.

The choice of the error bound depends on wavelength and array geometry. For the localization of the 2.083-Hz signal at GERESS, we applied an error bound of 100 m in equation (A7) and found 45 averaging pairs. Simulations with synthetic data showed that this averaging makes MUSIC much more robust to correlated signals and to errors in estimating the number of signals (Baisch, 1997).

Institut für Geophysik
Universität Bochum
44780 Bochum, Germany
E-mail: bokelmann@geophysik.ruhr-uni-bochum.de,
baisch@geophysik.ruhr-uni-bochum.de

Received 11 June 1998.